

Design and experiment of the components for soil flow direction control of hilling machine based on EDEM

Zhenwei Tong, Lianhao Li, Xiuli Zhang*, Yong Chen, Xiaochan Liu, Peilin Zhou, Yueqing Xia
(College of Mechanical and Electrical Engineering, Henan Agricultural University, Zhengzhou 450002, China)

Abstract: Cultivation and hilling are important steps in crop field management and provide an important guarantee of crop quality and quantity. With the aim of addressing how the soil flow direction of a traditional cultivation and hilling machine is difficult to control, and because it is difficult to achieve high ridge soil cultivation, among other issues, the components of the soil flow direction control of a hilling machine was designed. The components of the soil flow direction control consisted of a soil-feeding plough device, spiral knives and guide cover devices, etc. The design and analysis of the guiding parts for the two tools of the soil-feeding plough device and the spiral knife were performed to obtain an appropriate guide wall and helix angle. The guiding principle in the flow direction control components was analyzed. The design of the guide wall adopts the torsional columnar plough surface, and the elementary line angle changes from stable to increasing. The analysis of spiral milling showed that when the spiral angle is large, the milling effect is better. According to the discrete element method, the working part of the machine-soil interaction model was established. EDEM software was used to simulate the control components for the soil flow direction of the hilling machine for compound cutting. The design method with a two-factor comprehensive test was used to study the linear velocity along the outer part of the spiral knife and the influence of the forward velocity of machine of the implement on the soil cultivation effect. The results of the discrete element simulation showed that both the linear velocity along the outer part of the spiral knife and the forward velocity of the machine have extremely significant effects on the transportation of particles to the ridge top and the hilling thickness. Following multiple comparisons of the average hilling thickness with different linear velocities along with the outer spiral knife and different forward velocities of the machine, it is concluded that the performance of the machine is better when the linear velocity along the outer spiral knife is 3.01 m/s and the forward velocity of the machine is 0.7 m/s. The research conclusion had great theoretical value and practical significance for the design of the machine, which worked for cultivation and hilling.

Keywords: compound cutting, hilling machine, flow direction control, discrete element method, design

DOI: 10.25165/j.ijabe.20221503.5857

Citation: Tong Z W, Li L H, Zhang X L, Chen Y, Liu X C, Zhou P L, et al. Design and experiment of the components for soil flow direction control of hilling machine based on EDEM. *Int J Agric & Biol Eng*, 2022; 15(3): 122–131.

1 Introduction

Together, cultivation and hilling is an important step in crop field management and an important guarantee for crop quality and quantity. For vegetables, onions, tobacco, and other crops, cultivation in high ridges can increase soil permeability and benefit root growth. Medium tillage and soil cultivation components need soil-cutting tools and a flow control structure to work together and make the soil flow to the roots of high ridge crops. In the field covering cutting tools for medium-tillage soil, many studies on soil cutting have been performed using ANSYS, EDEM, and other software both nationally and abroad. Zhai et al.^[1] used

ANSYS/LS-DYNA to simulate the plough cultivation process, finding that the soil displacement decreased gradually from the contact point to the surrounding area. Xu et al.^[2] studied the process of cutting soil with a soil cutting knife from a grape mulching machine, and they established a mechanical model for cutting soil with a soil cutting knife and obtained the curve of the cutting force. Fang et al.^[3] studied the movement of soil during rotary tiller operation by using the discrete element method. The soil displacement was found to increase with the increase in the rotational speed. Jiang et al.^[4] used the SPH method to simulate the vibration cutting process of rotary tillage under compacted soil conditions. The vibrational cutting of soil had an obvious drag reduction effect. Sadek et al.^[5] studied the interaction process between bulldozers and soil by changing the micro-parameters of soil particles, and they proposed the selection range of parameters. Momozu et al.^[6,7] created a soil model by establishing the discrete element method, and they studied the effect of cutting tools under different conditions and the state of the soil movement. Asl et al.^[8,9] studied the mechanism of interactions between cutting tools and soil particles by establishing a mathematical model and a cutting tool model. Domestic studies have also been performed on the compound cutting of soil in China. Combined cutting tools, such as the plough and rotary tiller, subsoiling shovel and ridging cutter, rotary tiller, and screw cross cutter, have been used to complete this operation^[10-13]. The above research is primarily intended to exert a certain force on the soil to break and cut the soil, which can provide a reference for the soil cutting function of the

Received date: 2020-04-21 **Accepted date:** 2022-02-14

Biographies: **Zhenwei Tong**, Master candidate, research interest: agricultural mechanization engineering, Email: tongzhenwei917@163.com; **Lianhao Li**, Associate Professor, research interest: agricultural water-soil engineering, Email: lianhao8002@126.com; **Yong Chen**, Lecturer, research interest: design and performance test of agricultural machinery, Email: chen Yong@henau.edu.cn; **Xiaochan Liu**, Lecturer, research interest: dynamics of intelligent agricultural equipment system, Email: liuxiaochan@henau.edu.cn; **Peilin Zhou**, Lecturer, research interest: additive manufacturing technology, Email: zhoupeilin@henau.edu.cn; **Yueqing Xia**, Lecturer, research interest: material connection technology of key components of agricultural machinery, Email: xiayueqing2016@163.com.

***Corresponding author:** **Xiuli Zhang**, PhD, Professor, research interest: theory and method of agricultural equipment design. College of Mechanical & Electrical Engineering, Henan Agricultural University, Zhengzhou 450002, China. Tel: +86-13938553090, Email: zhangxiuli619@126.com.

soil flow mechanism.

In relation to the flow direction analysis, because of the complexity of the soil flow direction, many domestic scholars use discrete element simulation software for analyses and research^[14]. Many scholars have studied the installation height and structure of cutting tools, and they established a soil model using EDEM simulation software. The soil movement state during deep loosening was analyzed and studied according to the lateral disturbance range, soil swelling degree, soil disturbance coefficient, soil vertical accumulation angle, soil fragmentation degree and tillage resistance^[15-17]. Shi et al.^[18] used EDEM simulation software to design the structure and motion parameters for the core components of a throwing-type membrane-covering device. Cheng^[19] studied a rotary tiller potato cultivator and analyzed the movement track of soil particles when the machine was reversed. Zhang^[20] analyzed the throwing performance of a rotary tillage fertilizer seeder. When the rotary tillage blade was reversed, the soil was thrown forward or backward along the rotary tillage blade. Luo et al.^[21] studied the transverse throwing performance of a rotary tillage ditcher. It was concluded that the speed and installation mode of the ditching shovel had great influence on the throwing distance. The above analysis primarily indicates that the soil reaches a certain initial velocity to complete the spraying movement while lacking the guidance of special guiding mechanism, and it is difficult to engage in accurate high ridge soil cultivation. For the movement of other materials, Zong et al.^[22] used a kinematics analysis method and ADAMS simulation software to analyze the trajectory of materials in a combined rape-threshing device, and they completed the trajectory control of the materials by moving away from the components. Shi et al.^[23] guided the trajectory of the fertilizer particles through the structural design of the conical disc granular fertilizer spreader.

Based on the above background, a composite cutting method suitable for high ridge crop cultivation is proposed, and it can control the flow direction of soil at multiple levels. The combination of inclined cutting by a plough cutter and the inclined milling of a spiral soil-cultivating cutter is used to perform the soil-cultivating operations to complete the cutting and transportation of soil. Rolling friction is used instead of sliding friction to reduce the resistance of the operation and to achieve better results. In addition, the flow direction of soil during the soil-cultivating operation is controlled so as to make more soil particles flow to the ridge top. This is the purpose of cultivating soil on high ridges. EDEM software is used to simulate the operation process of the soil plough and spiral soil knife, analyze the soil flow direction and optimize the flow control components, which provides a theoretical basis for the subsequent optimization of the soil plough^[24,25].

2 Design for components of the soil flow direction control of the hilling machine

2.1 Structure and working principle for components of the soil flow direction control

The hilling machine is mainly composed of frame, hydraulic transmission system, ridge distance adjusting device, depth limiting device, leaf protection device and soil flow control components, as shown in Figure 1. The hilling machine used is connected to the tractor rear by a three-point suspension. When the tractor moves forward, the components of the soil flow direction control complete the cutting, guiding, and conveyance of the soil, and it completes the soil cultivation operation process^[26]. As shown in Figure 2,

the components of the soil flow direction control from the hilling machine primarily consist of a plough device for feeding and distributing the soil, spiral knife, guiding cover device, side panel, supporting plate, and ridge shape adjusting device. θ is the inclination angle of the spiral knife, and the adjusting range is 50° - 70° . A_1 is the external diameter distance of the spiral knife cutter axis from the outer edge distance of the guide cover device, and the distance is 10 mm.

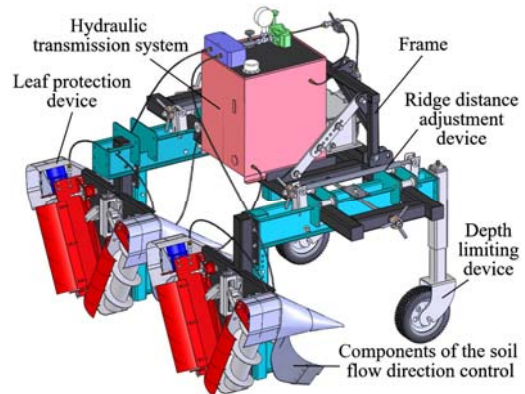
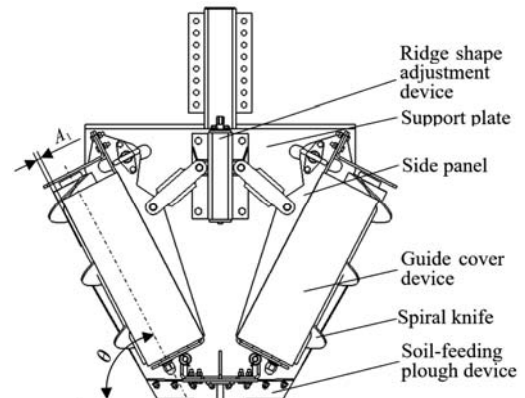


Figure 1 Structural diagrams of the hilling machine

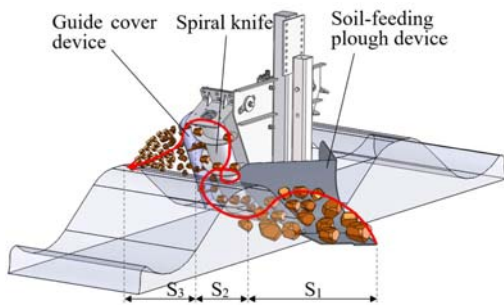


Note: θ is the inclination angle of spiral knife, ($^{\circ}$); A_1 is the external diameter distance of spiral knife cutter axis from outer edge distance of guide cover device, mm.

Figure 2 Structural diagrams of components from the soil flow control of the hilling machine

As shown in Figure 3, when the components of the soil flow control of the hilling machine are working, the plough device for feeding and distributing soil begins to work first, completes the oblique cutting of the ridge and furrow soil, divides the ridge and furrow soil into two helical soil-cultivation knives, provides the first soil transportation, and completes the first control of the soil cultivation amount and the flow direction of the soil, as shown in Figure 3, Section S_1 . The rotation of the spiral knife provides the second cutting transport for the furrowed soil and ridge side soil conveyed by the plough device for feeding and distributing the soil, which completes the second control of the soil flow direction, as shown in Section S_2 of Figure 3. Finally, the soil conveyed upward by the spiral knife is thrown to the ridge top under the action of an external guide cover device to complete the third control of the soil flow direction, as shown in Section S_3 of Figure 3. Through compound cutting and three soil flow control repetitions, the components of the soil flow control ensure that the soil is transported to the roots of the crops accurately, reduce damage to crop seedlings, complete the soil cultivation process, and simultaneously order the soil particles from large to small, so as to meet the requirements of the soil fragmentation rate. The

complete trajectory of soil movement is shown in the red trajectory in Figure 3.



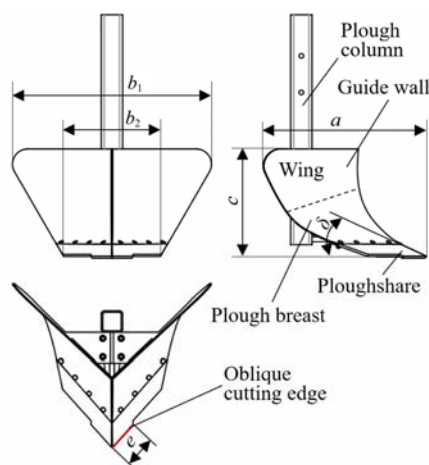
Note: S_1 is the guide section of lough device for feeding and distributing soil; S_2 is the guide section of spiral knife; S_3 is the guide section of guide cover device.

Figure 3 Structural diagrams of flow control in the hilling machine

2.2 Structural design and soil kinematics analysis for components of soil flow control

2.2.1 Design and analysis of soil feeding plough

As shown in Figure 4, the soil-feeding plough device is composed of a ploughshare, guide wall, and plough column. The guide wall can be divided into a chest and a wing. The plough column and guide wall are assembled in combination to facilitate replacement. The front part of the ploughshare is raised, and the cutting edge is not perpendicular to the direction of the cutting motion obliquely, leading to oblique cutting, reducing the impact, and stabilizing the process of cutting soil by the soil-feeding plough^[27]. To facilitate the control of the soil flow direction, the guide wall surface was designed with a gentle crest and low distortion, which is beneficial to the upward sliding of soil along the surface; the guide wall surface has a longer wing and larger distortion, which is convenient for lateral bulldozing and pushes the soil to both sides of the soil-feeding plough^[28]. In accordance with the agronomic requirements of crop cultivation and the parameters of the soil ridge, the length of the apex along the oblique cutting edge to the apex behind the guide wall (a) is 500 mm; the width of the guide wall (b_1) is 600 mm; the base width of the soil-feeding plough (b_2) is 320 mm; the height of the soil-feeding plough (c) is 350 mm; the oblique cutting edge length of ploughshare is (e) 300 mm. The rake angle of the soil-feeding plough (δ) is 30° , which is helpful in cutting soil.



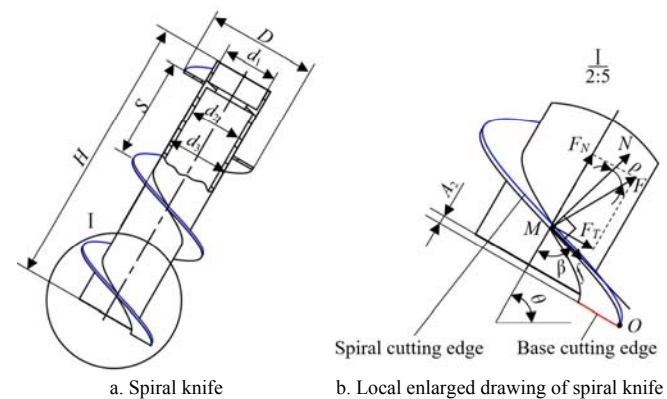
Note: a is the length of the apex of the oblique cutting edge to the apex behind the guide wall, mm; b_1 is the width of guide wall, mm; b_2 is the base width of soil-feeding plough, mm; c is the height of soil feeding plough, mm; e is the oblique cutting edge length of ploughshare, mm; δ is the rake angle of soil-feeding plough, ($^\circ$).

Figure 4 Structural diagrams of the soil-feeding plough device

Using the above design, the soil cutting and first guiding control are accomplished through the following three work processes: 1) the oblique cutting edge and the tibial cutting edge of the soil feeding plough cut the ridge and furrow soil along the horizontal and vertical planes, respectively; 2) the soil being cut is lifted and turned under the action of the ploughshare surface and the guiding wall; 3) the reversed soil moves to the rear side under the direction of the plough wing.

2.2.2 Design and analysis of the spiral knife

During spiral milling, the spiral knife is the primary component of spiral milling by the hilling machine. The structure of the spiral knife is shown in Figure 5. The spiral cutting edge and the base cutting edge work together to finish the soil milling, and the helical blade completes the soil guiding work. During the operation of the spiral knife, the M -point soil is subjected to the normal thrust (N) of the helical blade of the spiral knife and the friction (f) between the helical blade, the combined force (F) of the normal thrust (N) and the friction force (f) is F , the combined force (F) generates in the axial direction of the spiral knife is F_N , and the combined force in the radial direction of the spiral knife is F_T . The angle between the force (F) and the normal thrust (N) is the friction angle (ρ) of the soil at point M ^[29,30], and the angle between the tangent of the outer edge and the axis of the tool is the helix angle (β). The radial force and the axial force are different for materials with different helical angles. When the helix angle is large, the radial force (F_T) produced by the spiral knife on the material is small, and the torque it produces is small; moreover, the material needs a longer path of movement to rise and has better directivity and accommodation performance, which is conducive to the upward transportation of the material.



Note: M is milling point; O is base cutting edge vertex; H is the axis length of spiral knife, mm; S is the pitch of spiral knife, mm; D is the outer diameter of helical blade of spiral knife, mm; d_1 is the end diameter of spiral knife cutter axis, mm; d_2 is the inside diameter of spiral knife cutter axis, mm; d_3 is the external diameter of spiral knife cutter axis, mm; A_2 is the length of the helical blade beyond the end of spiral knife cutter axis, mm; β is the helix angle of spiral knife, ($^\circ$); ρ is the friction angle of soil particles, ($^\circ$); N is the normal force of helical blades on soil, N; f is the friction force of soil at milling point M , N; F is the force of cutter on soil at milling point M , N; F_T is the horizontal forces of F , N; F_N is the vertical components of F , N.

Figure 5 Structural diagrams of the spiral knife

$$\begin{cases} F_N = F \sin(\beta - \rho) \\ F_T = F \cos(\beta - \rho) \end{cases} \quad (1)$$

$$\begin{cases} \rho = \arctan \mu \\ \beta = \frac{\pi}{2} - \arctan \frac{S}{2\pi R} \end{cases} \quad (2)$$

where, μ is the friction coefficients between the soil particles and helical blades; S is the pitch of the helical soil knife, mm; R is the radius of the helical blade, in mm; ρ is the friction angle, ($^\circ$); β

is the helical angle of helical soil knife, (°).

To achieve the purpose of upward soil transportation along with the spiral knife, it is necessary to ensure that the normal thrust of soil particles in the axial direction is greater than the resistance of the soil in the axial direction.

$$N \cos\left(\frac{\pi}{2} - \beta\right) > f \cos \beta \quad (3)$$

$$f = \mu N = N \tan \rho \quad (4)$$

It is concluded that helix angle β should satisfy the following conditions:

$$\beta > \rho$$

The friction coefficient between the soil and carbon steel ranges from 0.3 to 0.6. When the maximum value of the friction coefficient is 0.6, the friction angle ρ is 31°; that is, the friction angle β is more than 31°.

According to the equation for calculating the pitch of the helical blade:

$$S = K_1 D \quad (5)$$

where, K_1 is the proportional coefficient, 0.8-1.0^[31].

According to the agronomic requirements of soil cultivation, soil characteristics and the design characteristics of spiral milling conveyance, the ratio coefficient K_1 is 0.94, and pitch S of the spiral knife is 178 mm. The helix angle β is

$$\beta = 1 - \arctan \frac{S}{\pi D} \quad (6)$$

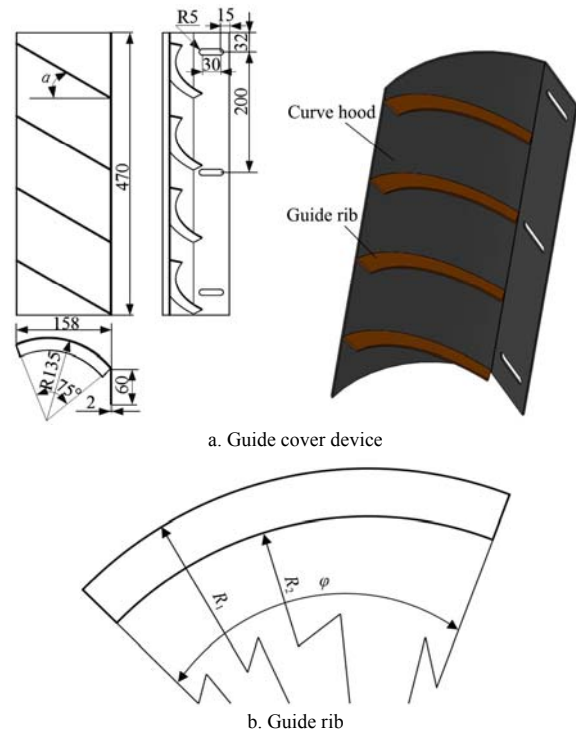
After the calculation, the helical angle β is 73.4^[32,33], which meets the requirement that it be larger than the external friction angle of the soil. Moreover, when the spiral knife works, it is engaged in unilateral milling, and the larger friction angle meets the requirement for reducing power consumption.

The interior design of the spiral knife has a hollow structure, which can reduce the quality of the entire machine. The spiral knife adopts a single-line solid helical structure^[34]. The helical blade of the spiral knife is stamped with a 4 mm thin steel plate and then welded to the helical shaft. According to the agronomic requirements of soil cultivation, the height H of the helical knife axis is 490 mm, the outer diameter D of the helical blade is 190 mm^[35], the inner diameter d_2 of the helical knife axis is 98 mm, and the outer diameter d_3 is 108 mm. The inner diameter d_1 of the helical knife axis is 100 mm because flanges need to be connected at both ends of the helical knife. According to the characteristics of helical milling, distance A_2 of the helical blade on the spiral knife is 5 mm, which ensures that when the spiral knife rotates at high speed, point O of the bottom cutting edge on the spiral knife contacts the soil first, so as to reduce the power consumption.

2.2.3 Design and analysis of the guide cover device

As shown in Figure 6a, the guide cover device consists of a curved hood and guide ribs. The circular groove is arranged on the curved hood to ensure that the distance between the inner part of the curved hood and the outer edge of the spiral blade of the spiral knife is adjusted over a range of 40-60 mm. Combined with the adjustment range of the ridge angle, the guide rib will be horizontal when the guide cover device is installed outside the spiral knife. When the guide cover device is placed vertically, the angle α between the guide rib and the horizontal plane will be 30°. The structure of the guide rib is circular, as shown in Figure 6b, and the center angle of the guide rib is 67°. According to the analysis of the soil characteristics and the soil capacity of the guide ribs, when the width of the guide ribs is larger, the soil accumulates too much on the guide ribs, and the friction increases, which makes

it difficult to guide. When the width of the guide ribs is too small, the guide ribs can only break the soil, but they cannot achieve a guiding effect. When considered comprehensively, the width of the guide rib is designed to be 20 mm, the external radius R_1 of the guide rib is 167 mm and the internal radius R_2 is 147 mm.



Note: α is the inclination angle of guide rib, (°); ϕ is the central angle of guide rib, (°); R_1 is the external radius of guide rib, mm; R_2 is the internal radius of guide rib, mm.

Figure 6 Structural diagrams of the guide cover device

3 Experiments and analysis of the discrete element simulation

The discrete element method (DEM) is a numerical analysis method proposed by Cundall in 1971^[36]. The basic idea of the discrete element method is to simplify the particle population into a collection of particles with a certain shape and mass, and artificially add contact between particles and between particles and boundaries. A certain contact mechanics model between boundaries and parameters in the model is used to consider the contact between particles and between particles and boundaries and the different physical and mechanical properties of particles and boundaries^[37,38].

Using the discrete element simulation software EDEM, an interaction model between the working parts of the machine and the soil was established. The field operation status of the soil-raising machine was simulated under normal working conditions. The factors affecting the performance of the machine were analyzed and the appropriate parameters were obtained, which laid the foundation for the subsequent optimization of the machine and the verification of the field experiment.

3.1 Experimental design

The components of the soil flow direction control of the hilling machine include the control of the soil flow direction for the first layer with the soil-feeding plough device as the primary part, the control of the second soil flow direction with the spiral knife as the primary part, and the control of the third soil flow direction with the guide cover device as the primary part. This study primarily analyses the influence of the two linear velocity factors along the

outer part of the spiral knife (A) v_0 and the forward velocity of machine (B) v_m on the soil-cultivating effect of the hilling machine. Among these factors, the forward velocity of the machine is provided by the tractor, and the linear velocity along the outer spiral knife is supplied by a separate hydraulic system to the power of the hydraulic motor, which is converted from the speed n of the hydraulic motor. Under the same other conditions, the two-factor comprehensive test design method was used to test the linear velocity along the outer spiral knife (A) v_0 and the forward velocity of machine (B) v_m are set as listed in Table 1.

Table 1 Factors and settings of the simulation experiments

Factors	Settings				
A: Linear velocity along the outer spiral knife $v_0/m \cdot s^{-1}$	0.50	1.76	3.01	4.02	5.02
B: Forward velocity of machine $v_m/m \cdot s^{-1}$	0.30	0.50	0.70	0.90	1.10

3.2 Method steps

3.2.1 Establishing a model of the hilling machine

To simplify the computer calculations, the whole machine was simplified, and the other components are hidden except for the soil-feeding plough device, the spiral knife, the bracket, and the guide cover device. SolidWorks, a three-dimensional drawing software, was used to model the entirety of the machine. Because the entire machine is too large and the size of the computer simulation is too large, the entity model is reduced by 4 times proportionally, and it is imported into EDEM software in step file format. According to the trial manufacturer characteristics of the physical prototype, the material attributes of the bracket and guide cover device are 45 steel, and the material attributes of the soil-feeding plough device and the spiral knife are 16 manganese steel. The simulation model parameters are shown in Table 2. The acceleration of gravity is set to 9.81 m/s^2 .

Table 2 Simulation model parameters

Parameters	Data	
Steel 45	Poisson's Ratio	0.310
	Shear Modulus/Pa	7.0×10^{10}
	Density/kg·m ⁻³	7800
Steel 16Mn	Poisson's Ratio	0.253
	Shear Modulus/Pa	7.9×10^{10}
	Density/kg·m ⁻³	7865

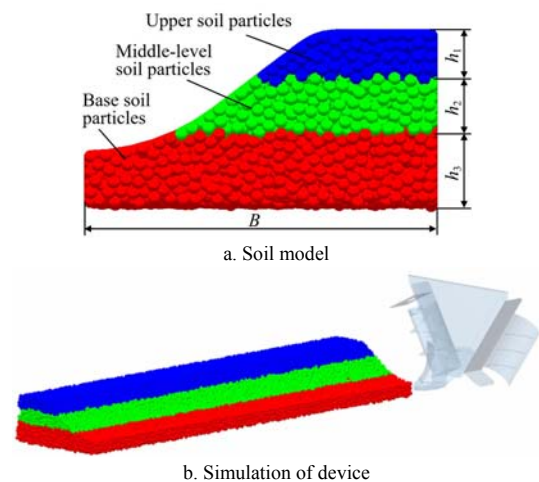
3.2.2 Establishment of a soil particle model

The soil's physical properties are closely related to the effect of mechanical soil cultivation. The soil moisture content, solidity and soil type have important effects on the simulation. To ensure that the simulation results are similar to the actual operation, the soil from the Guxing Town experimental field in Huiji District, Zhengzhou City, Henan Province was used as the research object; its physical parameters were measured, and its accumulation angle was calibrated by EDEM software for discrete element simulation. According to the experiment, the radius of the soil particle is 3 mm as the radius of the particle model. The Poisson's soil ratio is 0.35, the shear modulus is $1.0 \times 10^6 \text{ Pa}$, and the bulk density of the soil is 1300 kg/m^3 . Hertz-Mindlin with a bonding contact model was selected as the contact mechanics model between the soil particles^[39]. Because there are differences in the firmness of the ridge-furrow soil, ridge-side soil and ridge-top soil, different layers of soil models are set up. According to previous publications^[40-42], the coefficient of rolling friction, coefficient of static friction and coefficient of restitution between steel 45-soil particles, steel 16 manganese-soil particles and soil particles-soil particles were set up. The relevant parameters are listed in Table 3.

The soil ridge model was built in SolidWorks and imported into EDEM software in step file format. Three polygonal virtual planes were set up in EDEM to generate soil particles. The length of the filled soil model is 1000 mm. As shown in Figure 7a, the number of soil particles is 53 319. The height of the upper soil particles is 28 mm, the height of the middle soil particles is 27 mm, the height of the base soil particles is 34 mm, and the width of each half ridge is 175 mm. During the simulation process for the soil-cultivating machine, the model of the hilling machine was set on the ridge side for initial operation, as shown in Figure 7b. According to the operation of the hilling machine, the depth of the soil plough is 16 mm. To ensure the simulation's stability, a fixed time step was set at $5.10 \times 10^{-5} \text{ s}$ (10% of the Rayleigh time step), the total simulation time is 2.5 s, and the effective operation time is 1.8 s. Among these steps, the 1.8-2.5 s period is for the machine to leave the ridge shape, stop moving forward and wait for the particles to stabilize.

Table 3 Material contact parameters of the simulation

Parameters	45 steel-soil particle	16 manganese-soil particle	Soil particle-soil particle
Coefficient of rolling friction	0.04	0.03	0.20
Coefficient of static friction	0.50	0.50	0.54
Coefficient of restitution	0.28	0.28	0.20



Note: B is the width of soil model, mm; h_1 is the model height of upper soil particle, mm; h_2 is the model height of middle-level soil particle, mm; h_3 is the model height of base soil particle, mm.

Figure 7 Discrete element models

3.2.3 Simulation process for the hilling machine

The simulated operational state of the three-dimensional XYZ internal hilling machine is shown in Figure 8a, and the opacity of the parts of the adjusting machine was displayed at 0.3, to observe the state changes of the soil particles during cutting, conveyance and spraying. Figure 8b shows the working state of the soil cutting process with the soil feeding plough in the YOZ plane. When the machine moves forward along the Z-axis, the ploughshare part of the soil feeding plough first makes contact with the ridge and furrow soil and then begins cutting. With the machine moving forward, under the action of the guide wall on the soil-feeding plough, the ridge and furrow red particles and the ridge side green particles move backwards and upwards. Figure 8c is the working state of the cutting and transporting soil with the spiral knife in the XOY plane. The rotating spiral knife cuts and transports the soil transported by the soil-feeding plough and the uncut part of the soil transported by the soil-feeding plough, and it completes the soil-cultivating operation. The above two stages of the simulation are basically consistent with the actual working state.

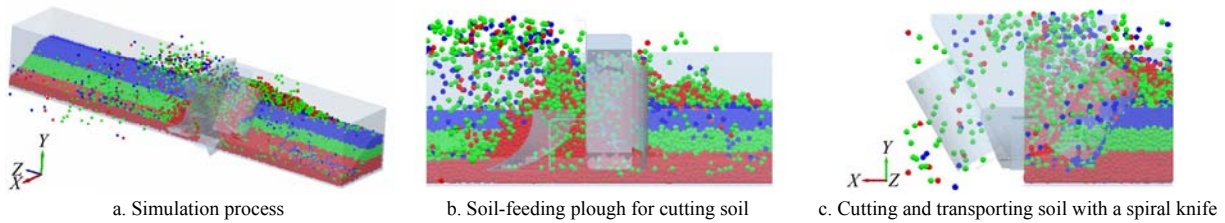


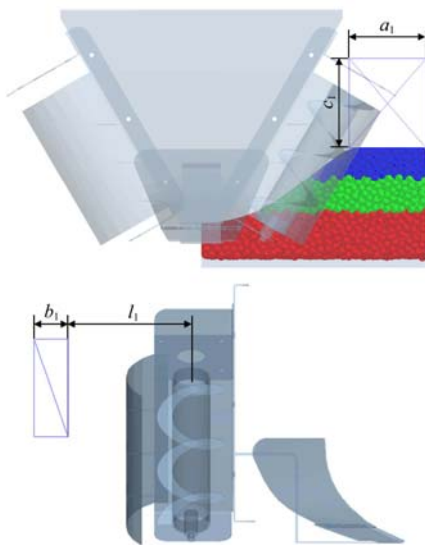
Figure 8 Simulated hilling operation in EDEM

3.3 Evaluation method for the hilling effect

The simulation experiment was completed. The number of particles transported to the ridge top under different conditions was counted by EDEM software, and the thickness of the soil on the ridge top was measured. The thickness of the soil on the ridge top refers to the thickness of the newly added soil on the original soil ridge after the operation is completed. The primary evaluation indexes are the total soil particles transported to the top of the ridge, the base soil particles transported to the top of the ridge, the thickness of the top of the ridge and the energy consumption of hilling machine. When more soil particles were transported to the ridge top, the effect of the soil cultivation is better; when more base soil particles were transported to the ridge top, the hilling machine uses the ridge and furrow soil to cultivate soil, which leads to water storage, moisture conservation and lodging resistance and meets the agronomic requirements of agricultural machinery.

3.3.1 Statistical method for the soil particle number on the ridge top

As shown in Figure 9, Geometry Bin 1 was set up by EDEM to move forward with the hilling machine. EDEM software was used to calculate the number of ridge top particles in the simulation process. The length, width, and height of Geometry Bin 1 are $a_1=60$ mm, $b_1=24$ mm, and $c_1=70$ mm, respectively, and the distance between Geometry Bin 1 and the center of the spiral knife is $l_1=87$ mm. The change in the particle number in Geometry Bin 1 at different times was obtained from EDEM software. The stable period of the particle number was selected and the average number of particles was taken.



Note: a_1 is the length of Geometry Bin 1, mm; b_1 is the width of Geometry Bin 1, mm; c_1 is the height of Geometry Bin 1, mm; l_1 is the distance between Geometry Bin 1 and axis of spiral knife, mm.

Figure 9 Setting the calculation area for Geometry Bin 1

3.3.2 Measuring method for hilling thickness

According to the change in the number of particles in Geometry Bin 1 for the calculation area, the stable time period for

the number of particles in the calculation area was selected. After the simulation, the calculation area for Geometry Bin 2 was set up to correspond to the particle stability region in the calculation area of Geometry Bin 1, as shown in Figure 10. The height of ridge top particles in Geometry Bin 2 was measured using the Ruler tool in EDEM software. The heights of 5 points in the stable region were selected equally and the average number was taken.

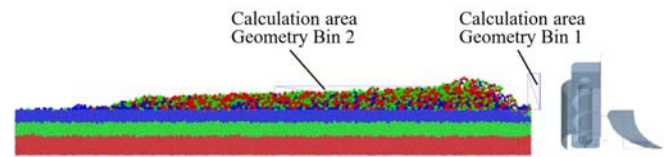


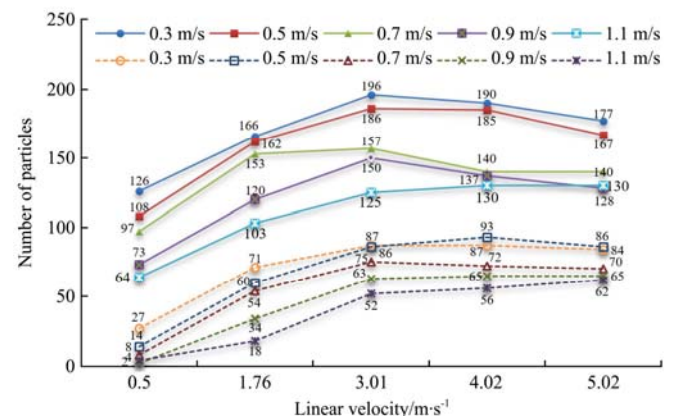
Figure 10 Setting the calculation area of Geometry Bin 2

3.3.3 Measuring method of energy consumption of machines

According to the design principle of the equipment, the energy consumption of hilling machine mainly comes from two aspects. One is the pressure on the plough to cut the soil; the other is the torque on the spiral knife. Therefore, the calculation method of the energy consumption of the implement is mainly the pressure on the plough and the torque on the spiral knife. In the EDEM software, select the region corresponding to the particle stability in geometry bin 1, respectively, derive the pressure on the plough and the torque on the spiral knife, and then carry out the analysis and calculation.

4 Results and analysis

Each group of experiments in the design scheme was repeated five times, and the average value was taken. The results are shown in Figures 11-14.



Note: Solid lines represent all soil particles, dotted lines represent base soil particles.

Figure 11 Effects of the linear velocity along the outer spiral knife and the forward velocity of the machine on the transportation of particles to the ridge top

Figure 11 shows that under the same forward velocity of the machine, with the increase of the linear velocity along the outer spiral knife, the total number of soil particles transported by the spiral knife to the top of the ridge first increases and then decreases.

When the linear velocity along the outer of spiral knife is 3.01 m/s and the forward velocity of the machine is 0.3 m/s, the maximum number of particles transported to the ridge top reaches 196. The number of red particles from the base to the top of the ridge increased first and then stabilized. When the linear velocity along the outer spiral knife reaches 3.01 m/s, the base particles conveyed to the top of the ridge are basically stable. At the same linear velocity along the outer spiral knife, the soil particles transported to the ridge top showed a decreasing trend with the increase in the forward velocity of machine. It is concluded that when the linear velocity along the outer spiral knife was low, the soil particles were subjected to a smaller axial force, larger radial force and fewer particles that move to a certain height. When the linear velocity along the outer spiral knife was high, the soil particles were subjected to a larger axial force, and the movement of the soil particles went farther. When the soil particles were thrown out, they had a larger initial velocity, which caused the soil particles to be thrown out the ridge top, and to fall more into the ridge and furrow.

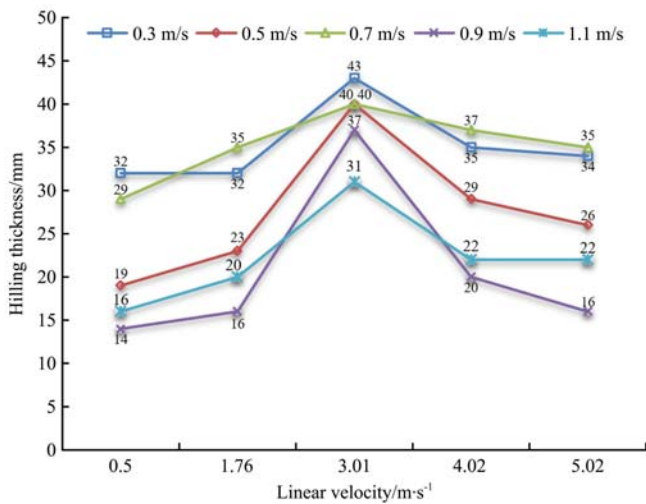


Figure 12 Effects of the linear velocity along the outer spiral knife and the forward velocity of the machine on the hilling thickness

The influence of different linear velocities along the outer spiral knife and the forward velocity of the machine on the hilling thickness is shown in Figure 12. The hilling thickness matches the number of particles conveyed by the spiral knife to the ridge top. When the linear velocity along the outer spiral knife is 3.01 m/s and the forward velocity of the machine is 0.3 m/s, the maximum is 43 mm. It was concluded that when the total number of particles is the same and the linear velocity along the outer of the spiral knife is the same, when the forward velocity of the machine is small, the spiral knife conveys more particles per unit time, so the hilling thickness is the largest. With the increase in the forward velocity of machine, during the process of upward transportation, due to the accumulation of soil particles in front, more particles have left the spiral knife before they can be transported to the ridge top in time, resulting in a lower hilling thickness and a poor soil cultivation effect.

The influence of the linear velocity along the outer of spiral knife and the forward velocity of the implement on the pressure of the soil-feeding plough and the torque of the spiral knife are shown in Figure 13 and Figure 14 respectively. It can be seen from Figure 13 that with the increase of the linear velocity along the outer of spiral knife, the pressure on the plough decreases. After the online speed is 1.76 m/s, the pressure change is not obvious.

When the linear speed is the same and the forward speed of the implement is 0.3 m/s, the pressure difference is large. At other forward speeds, there is little difference in pressure. It can be seen from Figure 14 that under the condition of the same forward speed of the implement, the torque of the spiral knife decreases with the increase of the linear speed; under the condition of the same linear speed, the torque increases with the increase of the forward speed. The analysis shows that when the linear velocity along the outer of spiral knife is low, the soil transportation is not timely, and the soil accumulation causes the coulter pressure to be high. When the spiral knife rotates, the soil is cut. Under the same forward speed, when the rotation speed of the spiral knife is low, the soil accumulates and compresses, when the linear velocity along the outer of spiral knife is lower, more soil will be cut per unit time, resulting in a large torque. With the increase of the linear velocity along the outer of spiral knife, the soil cutting is less per unit time, the soil is smoothly transported to the ridge, and the torque decreases.

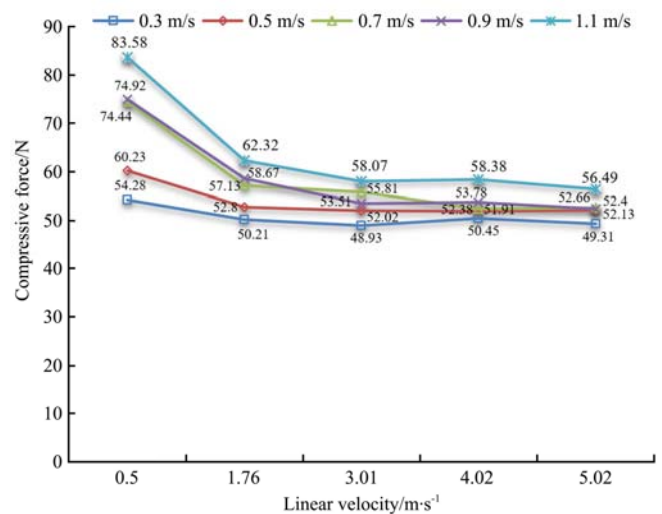


Figure 13 Effects of the linear velocity along the outer of spiral knife and forward velocity of machine on the compressive force of the soil-feeding plough

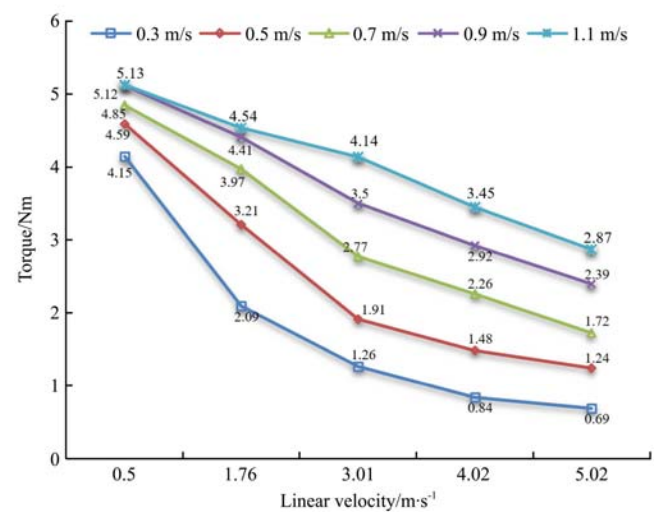


Figure 14 Effects of the linear velocity along the outer of spiral knife and forward velocity of machine on the torque of the spiral knife

To analyze the influence of the linear velocity along the outer spiral knife and forward velocity of machine on the effect of soil cultivation, the data in Figures 11 and 12 were analyzed by variance analysis, and the results are listed in Table 4.

Table 4 shows that the linear velocity along the outer spiral knife has a significant effect on the total number of soil particles transported to the ridge top, the number of base soil particles transported to the ridge top, and the hilling thickness ($p < 0.01$); the forward velocity of the machine has a significant effect on the total number of soil particles transported to the ridge top, the number of base soil particles transported to the ridge top and the hilling thickness ($p < 0.01$), which showed that the design scheme of the test is correct, and the analysis of the test results is of practical significance.

To obtain the ideal combination of working parameters for the hilling machine, multiple comparisons were made between the influence of the linear velocity along the outer spiral knife and the forward velocity of the machine on the hilling thickness. The results are listed in Tables 5 and 6.

From Table 5, it is clear that when the linear velocity along the outer spiral knife is 3.01 m/s, the difference in the average hilling

thickness is significantly higher than it is when the linear velocity is 0.5 m/s, 1.76 m/s, 5.02 m/s or 4.02 m/s. As shown in Table 6, when the forward velocity of the machine is 0.7 m/s, the difference in the average hilling thickness is significantly higher than that of the forward velocity at 0.9 m/s, 1.1 m/s and 0.5 m/s, but not significant when the forward velocity is 0.3 m/s.

In summary, when the linear velocity along the outer spiral knife is 3.01 m/s and the forward velocity of the machine is 0.3 m/s or 0.7 m/s, the hilling thickness is better. However, there was no significant difference in the average hilling thickness between 0.3 m/s and 0.7 m/s. Considering the working efficiency requirements of the hilling machine, 0.7 m/s is a better choice for the forward velocity of the machine. When the hilling machine is working, the linear velocity along the outer spiral knife is 3.01 m/s and the forward velocity of machine is 0.7 m/s, the hilling thickness is better and the soil-cultivating effect is better.

Table 4 Variance analysis of the experimental results

Experimental indexes	Source of variance	Sum of deviation square	Degree of freedom	Mean square	F value	p value	Significant
The transportation of all the soil particles to the ridge top	A	15 060.8	4	3765.2	62.2	<0.0001	***
	B	13 241.2	4	3310.3	54.7	<0.0001	***
	Error	968.0	16	60.5			
	Correct total	29 270.0	24				
The transportation of base soil particles to the ridge top	A	15 115.2	4	3778.8	97.9	<0.0001	***
	B	3919.6	4	979.9	25.4	<0.0001	***
	Error	617.2	16	38.6			
	Correct total	19 652.0	24				
Hilling thickness	A	750.6	4	187.7	23.8	<0.0001	***
	B	961.8	4	240.5	30.5	<0.0001	***
	Error	126.2	16	7.9			
	Correct total	1838.6	24				

Note: * means the difference is significant at the 0.1 level, ** means the difference is significant at the 0.05 level, *** means the difference is significant at the 0.01 level.

Table 5 Multiple comparisons of average hilling thicknesses with different linear velocities along the outer spiral knife

Velocity along the outer spiral knife $v_0/m \cdot s^{-1}$	Average \bar{x}_i	\bar{x}_i -22	\bar{x}_i -25.2	\bar{x}_i -26.6	\bar{x}_i -28.6
3.01	38.2	16.2**	13.0**	11.6**	9.6**
4.02	28.6	6.6**	3.4	2.0	
5.02	26.6	4.6*	1.4		
1.76	25.2	3.2			
0.50	22.0				

Note: * mean number is significantly different for the different levels of factors; ** mean number is extremely significantly different for the different levels of factors; and the mean number is not significantly different for the different levels of unmarked factors.

Table 6 Multiple comparisons of average hilling thicknesses with different forward velocities for the machine

Forward velocity of machine $v_m/m \cdot s^{-1}$	Average \bar{x}_j	\bar{x}_j -20.6	\bar{x}_j -22.2	\bar{x}_j -27.4	\bar{x}_j -35.2
0.7	35.2	14.6**	13.0**	7.8**	0
0.3	35.2	14.6**	13.0**	7.8**	
0.5	27.4	6.8*	5.2**		
1.1	22.2	1.6			
0.9	20.6				

5 Field experiment

To verify the accuracy of the design of the components for the soil flow direction control of the hilling machine based on the discrete element simulation, field experiments were performed under the given experimental conditions to verify the rationality of the design. Because the number of soil particles in the field cannot be measured, the ridge top hilling thickness was used as the evaluation index.

5.1 Experimental conditions and materials

In April 2019, the field performance experiment on the

components of the soil flow direction control of the hilling machine was performed in the Guxing Town experimental field of Huiji District, Zhengzhou City, Henan Province. The absolute moisture content of the soil is 15.3%, the ridge-side soil compactness is 2.3×10^5 Pa, the ridge furrow soil compactness is 3.5×10^5 Pa, and the soil bulk density is 1300 kg/m^3 . Before the experiment, the components of the soil flow direction control for the hilling machine were debugged, and the bottom of the soil-feeding plough device was adjusted to be 20 mm different from the bottom of the supporting plate in the vertical direction. The ridge distance adjustment device was adjusted to 1200 mm and the ridge shape

adjustment device was adjusted to 60°.

5.2 Experimental content and method

The field experiment on the components of the soil flow direction control of the hilling machine is shown in Figure 15. During the field experiment, the length of the preparation area is 5 m and the length of the measurement area is 20 m. The stable section of the middle section was selected to measure the hilling thickness. After the machine operation, the hilling thickness of wet soil on the ridge was measured, along the direction of the machine, 10 points were measured every 2 m, and the average value was calculated. At the beginning of the experiment, the linear velocity along the outer spiral knife was set at 3.01 m/s, and the forward velocity of the machine was 0.70 m/s.



Figure 15 Field experiment

5.3 Experimental results and analysis

For the field experiment on the components of the soil flow direction control of hilling machine, the measured value of the hilling thickness is listed in Table 7, and the average value of the hilling thickness was 142 mm. According to the agronomic requirements, the hilling thickness is within 15-150 mm, and the experiment results meet the agronomic requirements. The simulation experiment results showed that when the linear velocity along the outer spiral knife v_0 is 3.01 m/s, the forward velocity of machine v_m is 0.70 m/s, and the hilling thickness is 40 mm. Because of the reduction in the simulation model by four times, it is necessary to expand the simulation hilling thickness by four times, that is, the actual hilling thickness is 160 mm, or slightly larger than the field experiment results, with a relative error of 12.7%. The analysis showed that the characteristics of the soil, such as the moisture content, are different for the field experiment, and the external environment such as wind power and the vibration of machinery have great influence on the actual operation effect, which fails to reach the ideal hilling thickness. In addition, the reduction of the simulation model also has an impact on the experiment results.

Table 7 Measurement results for the hilling thickness

Measuring point	1	2	3	4	5	6	7	8	9	10
Hilling thickness/mm	118	147	162	142	139	142	161	149	120	140

6 Conclusions

1) In this study, the structure of the components of the soil flow direction control for a hilling machine was designed and analyzed. The guiding wall surface of the soil-feeding plough device was designed. The soil-cutting mechanism of the spiral knife and the force acting on the soil are analyzed. The geometric parameters of the soil feeding by the spiral knife were obtained.

2) Based on the discrete element method (DEM), a model of the interaction between the working parts of the machine tool and the soil was established. EDEM software was used to simulate the cutting and guiding of the soil by the soil feeding plough device,

the spiral knife, and the guiding cover device. The two-factor comprehensive experimental design method was adopted, and the linear velocity along the outer spiral knife and the forward velocity of the machine were used as the experimental factors to transport to the soil. The number of soil particles transported to the ridge top, the number of base soil particles transported to the ridge top, and the hilling thickness were the experimental indexes. The results of the variance analysis showed that both the linear velocity along the outer spiral knife and the forward velocity of the machine have significant effects on the grain conveyed to the ridge top and the hilling thickness. Through multiple comparative analyses of the average hilling thickness, it is concluded that when the forward velocity of machine is 0.7 m/s and the linear velocity along the outer of spiral knife is 3.01 m/s, the performance of the machine is more reasonable. At this time, the total number of soil particles on the top of the ridge and the number of base soil particles were 157 and 75, respectively.

3) The field experiment results showed that the hilling thickness is 142 mm, and the ideal hilling thickness is 160 mm, with a relative error of 12.7%. When considering the field experiment factors comprehensively, the field experiment results meet the design requirements and can meet the requirements of field soil cultivation.

Acknowledgements

This work was supported by the National Natural Science Foundation of China (Grant No. 52005167), the Scientific and Technological Research Project in Henan Province (Grant No. 202102110266), the Scientific and Technological Research Project in Henan Province (Grant No. 212102110235).

[References]

- [1] Zhai L X, Ji C Y, Ding Q S, Yu Y M. Analysis of distribution of displacement on soil surface in front of plow with FEM. *Transactions of the CSAM*, 2011; 42(10): 45–50. (in Chinese)
- [2] Xu G C, Huo S W, Zhao F Q. Study on the soil opening knife cutting soil process of grape covering machine. *Journal of Agricultural Mechanization Research*, 2017; 39(9): 31–35. (in Chinese)
- [3] Fang H M, Ji C Y, Farman A C, Guo J, Zhang Q Y, Chaudhry A. Analysis of soil dynamic behavior during rotary tillage based on distinct element method. *Transactions of the CSAM*, 2016; 47(3): 22–28. (in Chinese)
- [4] Jiang J D, Gao J, Zhao Y D, Willem H, Zhang X. Finite element simulation and analysis on soil rotary tillage with external vibration excitation. *Transactions of the CSAM*, 2012; 43(1): 58–62. (in Chinese)
- [5] Sadek M A, Chen Y. Microproperties calibration of discrete element models for soil-tool interaction. *ASABE Annual International Meeting*, 2014; 6: 3965–3978.
- [6] Momozu M, Oida A, Yamazaki M, Koolen A J. Simulation of a soil loosening process by means of the modified distinct element method. *Journal of Terramechanics*, 2002; 39(4): 207–220.
- [7] Tamás K, Jóri I J, Mouazen A M. Modelling soil-sweep interaction with discrete element method. *Soil and Tillage Research*, 2013; 134: 223–231.
- [8] Asl J H, Singh S. Optimization and evaluation of rotary tiller blades: Computer solution of mathematical relations. *Soil and Tillage Research*, 2009; 106(1): 1–7.
- [9] Shrivastava A K, Datta R K. Effect of different size and orientation of rectangular rotary blades on quality of puddling. *Journal of terramechanics*, 2006; 43(2): 191–203.
- [10] Qin K, Ding W M, Fang Z C, Du T T, Zhao S Q, Wang Z. Design and experiment of plowing and rotary tillage combined machine. *Transactions of the CSAE*, 2016; 32(16): 7–16. (in Chinese)
- [11] Bao P F, Wu M L, Guan C Y, Luo H F, He Y M, Xiang W. Design of plow-rotary style ditching and ridging device for rapeseed seeding. *Transactions of the CSAE*, 2017; 33(20): 23–31. (in Chinese)

- [12] Lin J, Wang L, Li B F, Tian Y, Bo H M, Ma T. Design and test of 2ZZ-3 type deep scarification-terrace ridge-fertilization combine intertill machine. *Transactions of the CSAE*, 2016; 32(24): 9–17. (in Chinese)
- [13] Zhang X M, Xia J F, Zhang J M, He X W, Liang S F, Zhang S, et al. Working performance experiment of combination blade roller for straw returning in paddy field and dry land. *Transactions of the CSAE*, 2016; 32(9): 9–15. (in Chinese)
- [14] Matin M A, Fielke J M, Desbiolles J M A. Torque and energy characteristics for strip-tillage cultivation when cutting furrows using three designs of rotary blade. *Biosystems Engineering*, 2015; 129: 329–340.
- [15] Wang X Z, Yue B, Gao X J, Zheng Z Q, Zhu R X, Huang Y X. Discrete element simulations and experiments of disturbance behavior as affected by mounting height of subsoiler's wing. *Transactions of the CSAM*, 2018; 49(10): 124–136. (in Chinese)
- [16] Asaf Z, Rubinstein D, Shmulevich I. Determination of discrete element model parameters required for soil tillage. *Soil and Tillage Research*, 2007; 92(1-2): 227–242.
- [17] Ma Y J, Wang A, Zhao J G, Hao J J, Li J C, Ma L P, et al. Simulation analysis and experiment of drag reduction effect of convex blade subsoiler based on discrete element method. *Transactions of the CSAE*, 2019; 35(3): 16–23. (in Chinese)
- [18] Shi L R, Yang X P, Zhao W Y, Sun W, Li R B, Sun B G. Design and test of potato combine seeder with throwing and covering soil on film edge. *Transactions of the CSAM*, 2018; 49(6): 129–137. (in Chinese)
- [19] Cheng Y M. The ridging performance analysis & optimization of ridging device of potato cultivator. Master dissertation. Chengdu: Xihua University, 2017; 72p. (in Chinese)
- [20] Zhang Y L. Simulation and experimental study throwing soil performance of reversal cultivated land and fertilization seeder based on DEM. Zhenjiang: Jiangsu University, 2012. (in Chinese)
- [21] Luo H F, Guan C Y, Tang C Z, Chen S Y, Wu M L, Xie F P. Experimentation on the performance of soil lateral throwing of rotary-cultivated ditchers. *Journal of Hunan Agricultural University (Natural Sciences)*, 2006; 4: 441–444. (in Chinese)
- [22] Zong W Y, Liao Q X, Huang P, Li H T, Chen L. Design of combined rape threshing device and analysis of rape cane movement trail. *Transactions of the CSAM*, 2013; 44(Supp2): 41–46. (in Chinese)
- [23] Shi Y Y, Chen M, Wang X C, Odhiambo M O, Weimin D. Numerical simulation of spreading performance and distribution pattern of centrifugal variable-rate fertilizer applicator based on DEM software. *Computers and electronics in agriculture*, 2018; 144: 249–259.
- [24] Mudarisov S G, Gabitov I I, Lobachevsky Y P, Mazitov N K, Rakhimov R S, Khamaletdinov R R, et al. Modeling the technological process of tillage. *Soil and Tillage Research*, 2019; 190: 70–77.
- [25] Ucgul M, Fielke J M, Saunders C. 3D DEM tillage simulation: Validation of a hysteretic spring (plastic) contact model for a sweep tool operating in a cohesionless soil. *Soil and Tillage Research*, 2014; 144: 220–227.
- [26] Zhang X L, Tong Z W, Li L H, Li Y J, Hou C P, Xia Y F. Design and experiment of tobacco hilling machine for compound cutting. *Transactions of the CSAM*, 2018; 49(9): 73–81. (in Chinese)
- [27] Luo Z W, Zhao W X, Jiao L, Gao S F, Liu Z B, Yan P, et al. Cutting force modeling in end milling of curved geometries based on oblique cutting process. *Journal of Mechanical Engineering*, 2016; 52(9): 184–192. (in Chinese)
- [28] Mattetti M, Varani M, Molari G, Morelli F. Influence of the speed on soil-pressure over a plough. *Biosystems Engineering*, 2017; 156: 136–147.
- [29] Xiao H R, Zhao Y, Ding W Q, Mei S, Han Y, Zhang Y, et al. Design and experiment on blade shaft of 1KS60-35X type orchard double-helix trenching and fertilization machine. *Transactions of the CSAE*, 2017; 33(10): 32–39. (in Chinese)
- [30] Sun G D, Ma X, Qi L, Lu F Y, Chen L T, An P, et al. Design and experiment of the screw device for mud lifting and conveying. *Journal of Agricultural Mechanization Research*, 2018; 40(6): 86–90. (in Chinese)
- [31] Gong Z Q. The experimental study on rheology of silage-corn stalk in the mechanized spiral dense forming process. PhD dissertation. Beijing: China Agricultural University, 2017; 116p. (in Chinese)
- [32] Wang S W, Li S J, Zhang Y L, Zhang C, Chen H, Meng L. Design and optimization of inclined helical ditching component for mountain orchard ditcher. *Transactions of the CSAE*, 2018; 34(23): 11–22. (in Chinese)
- [33] Li Y W, Zhang G Y, Zhang Z, Zhang Y, Hu T D, Cao Q Q. Development of low power-consumption multi-helical rotavator for small vertical-shaft deep-cultivator. *Transactions of the CSAE*, 2019; 35(4): 72–80. (in Chinese)
- [34] Li H T, Wan X Y, Xu Y, Jiang Y J, Liao Q X. Clearance adaptive adjusting mechanism for header screw conveyor of rape combine harvester. *Transactions of the CSAM*, 2017; 48(11): 115–122. (in Chinese)
- [35] Li Y Z, Guo J X, Zhang L, Liu X F, Yang H M, Zhang J X. Improved design and simulation analysis of screw conveyor system for 4FY-0.8B mobile biomass densification briquetting vehicle. *Journal of Chinese Agricultural Mechanization*, 2016; 37(12): 131–135. (in Chinese)
- [36] Cundall P A, Strack O D L. A discrete numerical model for granular assemblies. *Geotechnique*, 1979, 29(1): 47–65.
- [37] EDEM. EDEM theory reference guide. DEMSolutions, Edinburgh, UK, 2011; 11p.
- [38] Wen Y Y, Liu M L, Liu R Z, Liu B, Shao Y L. Comparative study between numerical simulation by discrete element method and typical experimental research of particles. *China Powder Science and Technology*, 2015; 21(3): 1–5. (in Chinese)
- [39] Tekeste M Z, Balvanz L R, Hatfield J L, Ghorbani S. Discrete element modeling of cultivator sweep-to-soil interaction: Worn and hardened edges effects on soil-tool forces and soil flow. *Journal of Terramechanics*, 2019; 82: 1–11.
- [40] Qi J T, Meng H W, Kan Z, Li C S, Li Y P. Analysis and test of feeding performance of dual-spiral cow feeding device based on EDEM. *Transactions of the CSAE*, 2017; 33(24): 65–71. (in Chinese)
- [41] Ma S, Xu L M, Xing J J, Yuan Q C, Yu C C, Duan Z Z, et al. Development of unilateral cleaning machine for grapevine buried by soil with rotary impeller. *Transactions of the CSAE*, 2018; 34(23): 1–10. (in Chinese)
- [42] Ma Y J, Wang A, Zhao J G, Hao J J, Li J C, Ma L P, et al. Simulation analysis and experiment of drag reduction effect of convex blade subsoiler based on discrete element method. *Transactions of the CSAE*, 2019; 35(3): 16–23. (in Chinese)